Voltage Control Method in Non-linear Dead-time Effect Region for Dual Active Bridge DC-DC Converter

Jun-ichi Itoh[1], Kengo Kawauchi[1], Hayato Higa[1], Hiroki Watanabe[1] and Keisuke Kusaka[1]
[1] Nagaoka University of Technology, Japan

***Abstract*-- This paper proposes a voltage control method for a Dual Active Bridge (DAB) converter with three-level operation in the dead-time effect region. The non-linear transmission power error is reduced by controlling the zero current phase to the dead-time or more because the non-linear error of the transmission power occurs when the inductor current reaches zero during the dead-time. In addition, the voltage control is operated under the linear region which is decided from the output current and the zero-voltage period. The validation of the proposed method is confirmed by a 2.3-kW prototype. In the experiments, the non-linear error in the transmission power is reduced by 76.3%. The linearity between a control variable and an output current is confirmed. In addition, a load step between two modes of three-level operation is achieved without the dc offset in the inductor current. Moreover, the RMS value of the inductor current is reduced by 50.2% compared with the conventional triangular modulation.**

***Index Terms*—Dual Active Bridge converter, Voltage control, Non-linear, Dead-time**

I. INTRODUCTION

Recently, DC micro-grid systems have been studied [1]-[5]. A power conversion efficiency is improved by applying DC micro-grid systems because the number of power conversion times is reduced. In order to compensate power variation of the high voltage DC-bus, an energy storage systems is applied [6]-[9]. The isolated bidirectional DC-DC converter is used for the energy storage systems to control power between battery and high voltage DC-bus safely. A dual active bridge (DAB) converter is applied to the energy storage systems because the DAB converter obtains high efficiency [10]-[15]. Especially, the zero voltage switching (ZVS) is achieved at the turn on state of switching devices. However, the DAB converter has several drawbacks; one is the error of the transmission power caused by the dead-time at medium load to light load which prevents the DAB converter from operating over wide load range. Compensation methods for the transmission power error have been proposed [16]-[17]. In [16]-[17], the error of the transmission power is compensated by the feedforward control which subtracts the dead-time from the command value of the phase-shift. However, this compensation method does not compensate an error of the transmission power due to voltage polarity reverse phenomenon [18]. The compensation method for the non-linear error of the transmission power has been proposed to solve this problem [19]. The non-linear error of the transmission power is suppressed by the zero-current period designed to dead-time or more in three-level mode.

On the other hand, the relationship between the control variable of the phase-shift and an output current is non-linear in the voltage control. Therefore, the gain of the PI controller is varied depending on the operation point. As the result, the controller design is complicated because the non-linear compensation in the voltage control is needed to achieve the desired response. In order to compensate non-linear effect in the voltage control, compensation methods have been proposed [17], [20]. In [17], the value of proportional gain of the PI controller is calculated every control cycle to vary the proportional gain dependently on the operating point. In addition, the error compensation of the transmission power owing to the dead-time is conducted by the feedforward control. Nevertheless, this method does not consider the non-linear dead-time effect. Meanwhile, the linearization method in the voltage control have been proposed for the DAB converter [20]. In [20], non-linear factor in the plant of the DAB converter is compensated by applying the linearization control [21]. However, the RMS value of the inductor current is increased because the inductor current is needed to be controlled by the triangular modulation (TRM).

This paper proposes a voltage control method in the non-linear dead-time effect region for the DAB converter. The voltage control is operated by three-level mode, where the relationship between the output current and control variable is linear. In particular, the non-linear error of the transmission power because of the dead-time is compensated by the three-level operation. The originality of this paper is to overcome two non-linear problem of the DAB converter to achieve the desired response in the voltage control.

This paper is organized as follows; the effect of the dead-time on the transmission power is explained in section II. Next, the compensation method for the nonlinearity in the transmission power is introduced in section III. In section V, the voltage control method in the region with non-linear dead-time effect is presented. Finally, the effectiveness of the voltage control method in

the dead-time effected region is confirmed by the experiments.

II. Dead-time Effect on Transmission Power

Figure 1 shows the DAB converter configuration. The DAB converter consists of an auxiliary inductor, a high frequency transformer, and two H-bridge inverters. Two H-bridge inverters generate a square wave voltage with a duty ratio of 50%. In the DAB converter, the phase-shift between primary and secondary transformer voltage controls the transmission power.

Figure 2 shows the typical operation waveforms without and with the dead-time effect, and figure 3 shows the state of the circuit in the voltage polarity reverse phenomenon. Without the dead-time effect, the phase-shift controls the transmission power introducing no error of the transmission power. According to Fig. 2 (a), the inductor current is introduced by (1) ignoring the magnetizing current and the parasitic capacitance. Moreover, the turn ratio of the high frequency transformer N is designed as one for simplifying the consideration.

$$i_L(\theta)=\begin{cases}\dfrac{V_{in}+V_{out}}{\omega L}\theta-\dfrac{1}{2\omega L}\{\pi V_{in}+(2\delta-\pi)V_{out}\} \\ \qquad for\quad (0\le\theta\le\delta) \\ \dfrac{V_{in}-V_{out}}{\omega L}(\theta-\delta)+\dfrac{1}{2\omega L}\{(2\delta-\pi)V_{in}+\pi V_{out}\} \\ \qquad for\quad (\delta\le\theta\le\pi)\end{cases} \quad (1),$$

where δ and L are a phase-shift between the primary transformer voltage v_{pr} and the secondary transformer voltage v_{se} and an auxiliary inductor value, $\omega$is a switching angular frequency, V_{out} and V_{in} are output voltage and input voltage. According to (1), the transmission power is introduced by following;

$$P=\frac{2}{2\pi}\int_0^{\pi}v_{pr}(\theta)i_L(\theta)d\theta=\frac{V_{in}V_{out}}{\omega L}\delta\left(1-\frac{|\delta|}{\pi}\right) \quad (2).$$

In contrast, the dead-time is necessary to avoid short circuit in the actual system. The non-linear error of the transmission power is caused when the inductor current reaches zero during the dead-time. Then, the inductor current is clamped to zero because two H-bridge inverters does not flow the current. In particular, all switching devices in the primary H-bridge inverter are turned off due to the dead-time. As the result, the secondary transformer voltage occurs in the primary side of the transformer. This phenomenon is called voltage polarity reverse phenomenon [18].

Figure 4 shows the boundary condition of the non-linear transmission power error. The non-linear error of the transmission power is caused by the voltage polarity reverse phenomenon when the inductor current reaches zero during the dead-time. Hence, the initial point of the voltage polarity reverse phenomenon is when the end point of the dead-time equals the zero cross timing of the inductor current. This condition of the phase-shift is given by (3) using (1) of $0\le\theta\le\delta$,

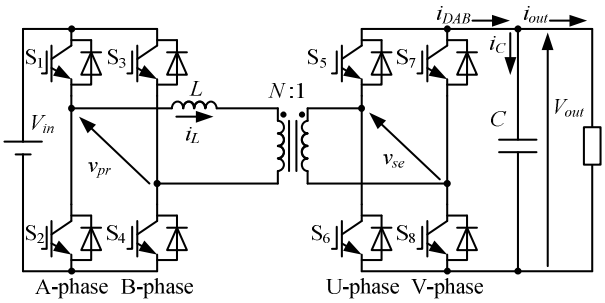

Fig. 1. Dual active bridge converter.

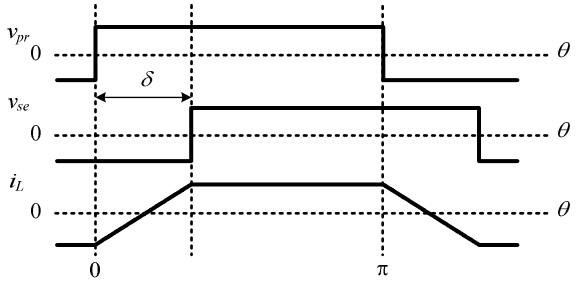

(a) Without dead-time.

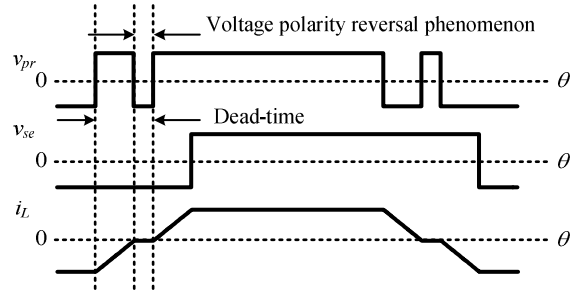

(b) With non-linear dead-time error.

Fig. 2. Traditional operation waveforms.

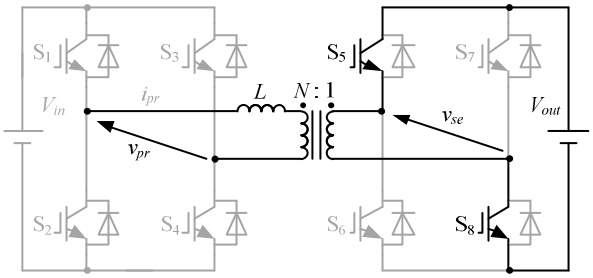

Fig. 3. Circuit in the voltage polarity reverse phenomeon.

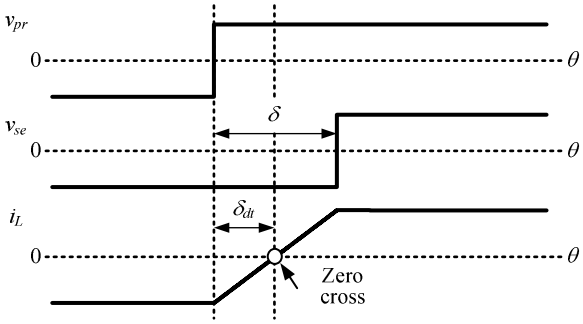

Fig. 4. Boundary condition of non-linear transmission power error.

$$\frac{V_{in}+V_{out}}{\omega L}\delta_{dt}-\frac{1}{2\omega L}\{\pi V_{in}+(2\delta-\pi)V_{out}\}\geq 0$$
$$\delta\leq(2\delta_{dt}-\pi)\frac{V_{in}}{2V_{out}}+\frac{1}{2}(2\delta_{dt}+\pi) \quad (3)$$

where δ_{dt} is the dead-time in the radian calculated as (4) using the dead-time T_{dt} and switching angular frequency ω,

$$\delta_{dt}=\omega T_{dt} \quad (4).$$

Figure 5 shows the effect of the voltage polarity reverse phenomenon on the transmission power when the input voltage V_{in} is same as output voltage V_{out}. According to (3), the starting point of the voltage polarity reverse phenomenon is $\delta = 2\delta_{dt}$. The error of the transmission power is increased accordingly to the decrease of the phase shift command because the width of the voltage polarity reverse is varied corresponding to the zero cross timing of the inductor current. The voltage polarity reverse phenomenon is stopped when the phase-shift command δ^* equals to the dead-time δ_{dt}. In this state, diodes does not conduct at the turn on timing of the IGBT, causing the dead-zone. The phase-shift command is canceled because the phase-shift command is smaller than the dead-time δ_{dt}.

III. Non-linear Error Compensation Method for Transmission Power

Figure 6 shows the proposed three-level operation. In the three-level operation, the transmission power is controlled by the three-variables: the zero voltage period of the primary side ε, the zero voltage period of the secondary side γ and the phase-shift δ. According to Fig. 6 (b), the zero voltage period is generated by circulating current. The three-level mode is considered under the condition of $V_{in} = NV_{out}$. In addition, the zero voltage period of each inverter are controlled as $\varepsilon = \gamma$ to generate the zero current phase ϕ. Note that the magnetizing current and the parasitic capacitance are not considered. At the steady state, the inductor current i_L at the switching moment is given by (5),

$$i_L(\theta)=\begin{cases}0 & (0\leq\theta\leq\varepsilon)\\ \frac{V_{in}}{\omega L}(\theta-\varepsilon) & (\varepsilon\leq\theta\leq\varepsilon+\delta)\\ \frac{V_{in}}{\omega L}\delta & (\varepsilon+\delta\leq\theta\leq\pi-\varepsilon)\\ \frac{V_{in}}{\omega L}(\pi-\varepsilon+\delta-\theta) & (\pi-\varepsilon\leq\theta\leq\pi-\varepsilon+\delta)\\ 0 & (0\leq\theta\leq\varepsilon)\end{cases} \quad (5).$$

According to (5), the transmission power is calculated as follows;

$$P=\frac{2}{2\pi}\int_0^{\pi}v_{pr}(\theta)i_L(\theta)d\theta$$
$$=\frac{V_{in}^2}{2\pi\omega L}\delta(2\pi-4\varepsilon-\delta) \quad (6).$$

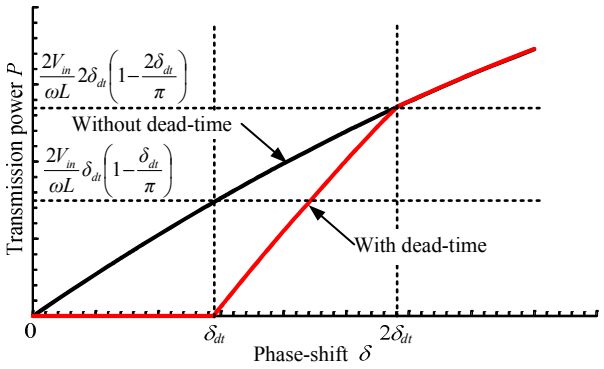

Fig. 5. Effect of the voltage polarity reverse phenomenon for transmission power.

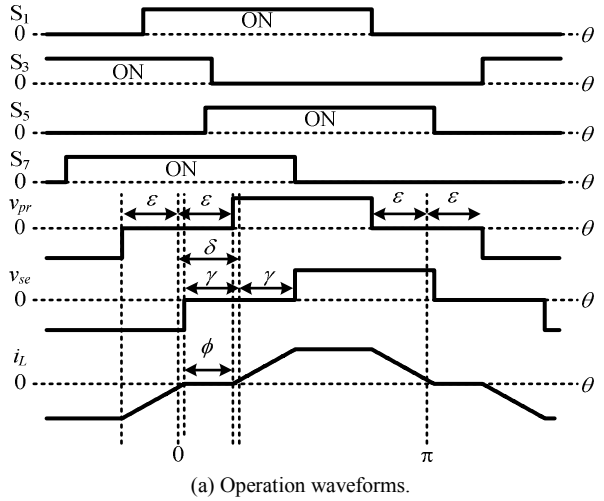

(a) Operation waveforms.

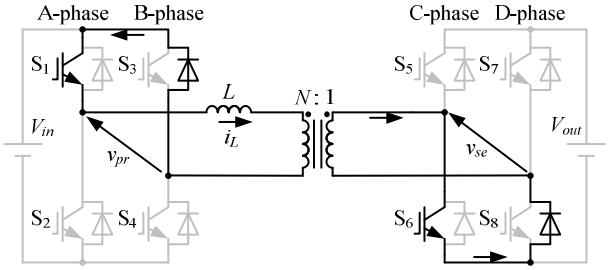

(b) Current flow during zero voltage period.

Fig. 6. Proposed three-level operation.

In order to control the three-level operation, pulses of each transformer voltage are needed to be overlapped. The condition of the three-level mode is expressed as follows;

$$2\varepsilon<\pi-\delta \quad (7).$$

In addition, the RMS value of the inductor current in the three-level mode is given by (8), derived from (5),

$$i_{L\_RMS}=\sqrt{\frac{2}{2\pi}\int_0^{\pi}i_{LI}(\theta)^2d\theta}$$
$$=\frac{V_{in}}{\omega L}\sqrt{\frac{1}{3\pi}(2\varepsilon-\pi)^2(3\delta-\pi+2\varepsilon)} \quad (8).$$

The voltage polarity reverse phenomenon is eliminated by controlling the zero current period ϕ to the dead-time δ_{dt} or more using the three-level operation because the voltage polarity reverse phenomenon is caused when the inductor current becomes zero during the dead-time. The

condition to avoid the voltage polarity reverse phenomenon is given by (9) shown in Fig. 6,

$$\varphi = 2\varepsilon - \delta \geq \delta_{dt} \tag{9}$$

Figure 7 shows the effect of the dead-time in the three-level operation. The duty of the transformer voltage of the primary side is decreased by the dead-time δ_{dt} because the inductor current does not flow the diode on the B-phase leg during the dead-time thanks to the zero- current period being longer than dead-time. Hence, duty compensation is necessary for the primary transformer voltage.

Figure 8 shows the compensation method of the decrease in the duty for the three-level operation. The decrease in the duty affects not only the phase-shift but also the zero voltage period of the primary side. Therefore, the duty compensation is needed for both phase-shift and the zero voltage period of the primary side. The duty compensation is introduced as follows;

$$\begin{cases} \delta^* = \delta + \dfrac{\delta_{dt}}{2} \\ \varepsilon^* = \varepsilon - \dfrac{\delta_{dt}}{2} \\ \gamma^* = \varepsilon \end{cases} \tag{10}$$

where ε^*, γ^*, and δ^* are the zero voltage period command of the transformer voltage of the primary side, the zero voltage period command of the transformer voltage of the secondary side, and the phase-shift command.

IV. Voltage Control Method in Non-linear Dead-time Effect Region

A. Conventional voltage control method

Figure 9 shows the conventional voltage control principle. The phase-shift command δ^* is generated by the PI controller in the conventional method. However, the plant of the DAB converter G_{DAB} has the non-linear factor. The relationship between the phase-shift δ and DAB output current i_{DAB} is expressed as (11) from (2) and $P = V_{out}i_{DAB}$,

$$i_{DAB} = \frac{V_{in}}{\omega L}\delta\left(1 - \frac{|\delta|}{\pi}\right) \tag{11}$$

According to (11), the relationship between the phase-shift δ and the DAB output current i_{DAB} is non-linear. Therefore, the control variable is not in proportion to the output current in the PI controller. Especially, the design of the gain is complicated because the non-linear error of the transmission power is caused at light load. Moreover, the DAB output current is varied by the voltage polarity reverse phenomenon. As the result, two types of the non-linearity occur at light load.

B. Conventional voltage control operation

Figure 10 shows the operation waveforms of the trapezoidal modulation (TRM). In the condition of $V_{in} = V_{out}$, the phase-shift δ is same as each zero voltage period

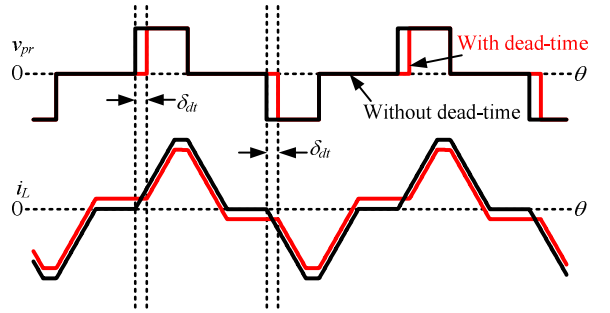

Fig. 7.Dead time effect for three-level operation.

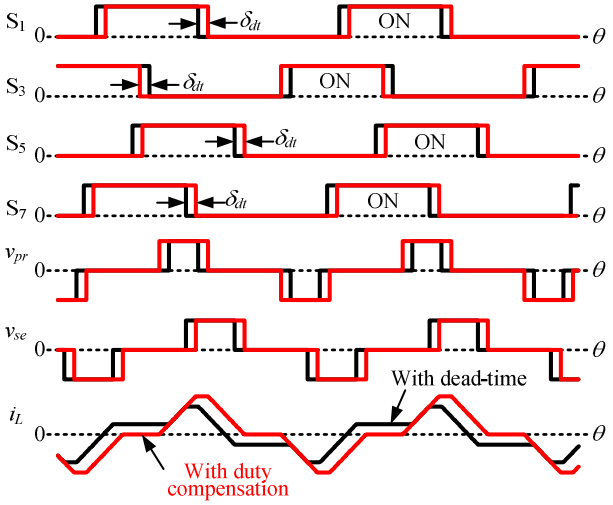

Fig. 8. Duty compensation method for three-level operation.

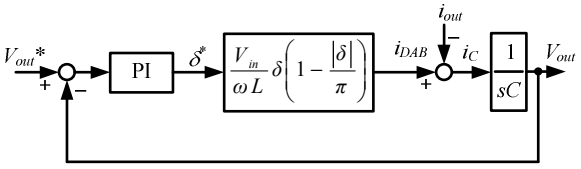

(a) Control block diagram.

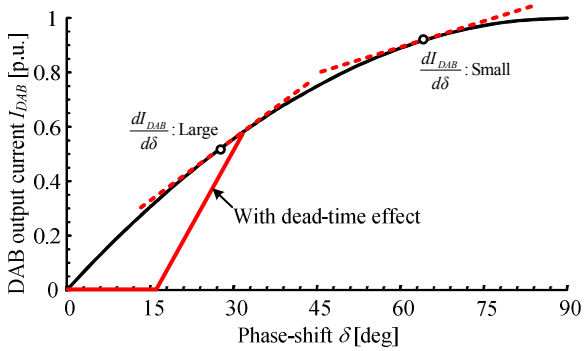

(b) Non-linearity between phase-shift and DAB output current.

Fig. 9. Conventional voltage control method.

ε and γ. At the steady state condition, the inductor current i_L at the switching moment as follows;

$$i_L(\theta) = \begin{cases} \dfrac{V_{in}}{\omega L}(\theta - \pi + 3\varepsilon) & (0 \leq \theta \leq \pi - 3\varepsilon) \\ 0 & (\pi - 3\varepsilon \leq \theta \leq \varepsilon) \\ \dfrac{V_{in}}{\omega L}(\theta - \varepsilon) & (\varepsilon \leq \theta \leq \pi - \varepsilon) \\ \dfrac{V_{in}}{\omega L}(2\pi - 3\theta) & (\pi - \varepsilon \leq \theta \leq \pi) \end{cases} \tag{12}.$$

According to (12), the transmission power in the TRM is given by (13),

$$P = \frac{2}{2\pi}\int_0^{\pi} v_{pr}(\theta) i_L(\theta) d\theta = \frac{V_{in}^2}{2\pi\omega L}(\pi - 2\varepsilon) \quad (13).$$

In addition, the RMS value of the TRM is introduced as follows;

$$i_{L\_RMS} = \sqrt{\frac{2}{2\pi}\int_0^{\pi} i_{LI}(\theta)^2 d\theta} = \frac{V_{in}}{\omega L}\sqrt{\frac{2}{3\pi}\left(\pi^3 - 6\varepsilon\pi^2 + 12\varepsilon^2\pi - 8\varepsilon^3\right)} \quad (14).$$

C. Proposed voltage control method

Figure 11 shows the proposed voltage control method. In order to eliminate the non-linear dead-time effect, the three-level operation is used. In the three-level operation, the relationship between control variables and the output current i_{DAB} is given by (15) from (6) and $P = V_{out}\, i_{DAB}$,

$$i_{DAB} = \frac{V_{in}}{2\pi\omega L}\delta(2\pi - 4\varepsilon - \delta) \quad (15).$$

According to (15), the relationship between the zero voltage period ε and the output current i_{DAB} is linear considering the phase-shift δ as constant value.

Next, the determination method of the phase-shift δ for the three-level mode is explained. In order to transfer the power with the non-linear error compensation method on the transmission power, multiple values of phase-shift δ are necessary to compensate entire region with the dead-time effect. In this paper, two phase-shifts are selected for achieving the maximum and minimum transmission power to reduce the operation modes. The maximum power is achieved when the zero voltage period is the shortest: (9) is established. By substituting (9) into (6), the transmission power is expressed by (16),

$$P = \frac{V_{in}}{2\pi\omega L}\left\{-\delta^2 + (-\delta_{dt} + 2\pi)\delta\right\} \quad (16).$$

In (7), the maximum power is obtained when the phase-shift δ becomes minimum. Therefore, the phase-shift for achieving the maximum power δ_{max} is given by (17) derived from (16),

$$\frac{d}{d\delta}\left\{-\delta^2 + (-\delta_{dt} + 2\pi)\delta\right\} = 0 \quad \delta_{\max} = \frac{1}{3}(\pi - \delta_{dt}) \quad (17)$$

In contrast, the minimum transmission power is obtained when $\delta = \delta_{dt} + \alpha$, where α is a margin to prevent the voltage polarity reverse phenomenon because this phenomenon occurs at $\delta = \delta_{dt}$. The margin α is needed to be design as small as possible because the circulating current increases as the margin α is larger. The margin α is determined as one clock of an FPGA (field-programmable gate array) when an FPGA is used for an experiment. The phase-shift is controlled by the clock

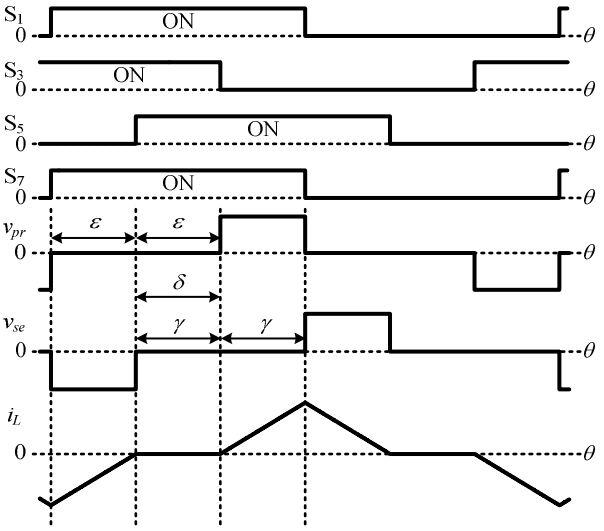

Fig. 10. Operation waveform of trapezoidal modulation.

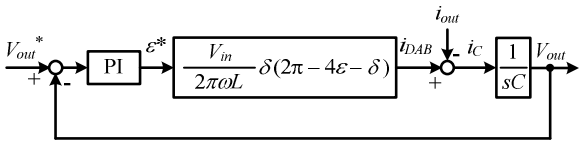

(a) Control block diagram.

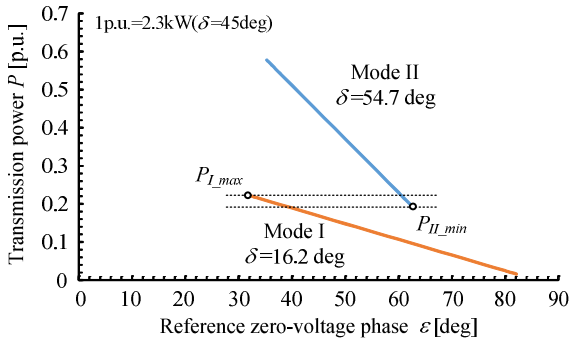

(b) Relationship between phase-shift and DAB output current.

Fig. 11. Proposed voltage control method.

period of FPGA. Therefore, the phase shift for achieving the minimum transmission power δ_{min} is given by (18),

$$\delta_{\min} = \delta_{dt} + \alpha \quad (18).$$

In the proposed method, the three-level mode I is applied with the phase-shift for achieving the maximum transmission power δ_{max}. On the other hand, the three-level mode II is applied with the phase-shift for achieving the minimum transmission power δ_{min}. The changing mode is conducted at the maximum transmission power in the three-level mode I P_{I_max} from mode I to mode II. Meanwhile, the mode changing from mode II to mode I is conducted at the minimum transmission power in the three-level mode II P_{II_min}. The maximum transmission power in the three-level mode I P_{I_max} is given by (19) from (6), (7), and (18),

$$P_{I\_\max} = \frac{V_{in}^2}{2\pi\omega L}(\alpha + \delta_{dt})(2\pi - 5\delta_{dt} - 3\alpha) \quad (19).$$

The minimum transmission power in the three-level mode II P_{II_min} is given by (20) from (6), (7), and (17),

$$P_{II\_\min} = \frac{V_{in}^{\ 2}}{18\pi\omega L}(\pi - \delta_{dt})^2 \qquad (20).$$

Figure 12 shows the control block diagram of the proposed method. The operation mode is decided by the transmission power calculated by the detected output current and the detected output voltage. The duty compensation is applied for the primary transformer voltage v_{pr}. Next, the phase-shift carriers of each leg is generated using the zero voltage period of each transformer voltage ε, $\gamma$and the phase-shift to operate the three-level operation.

V. Experimental Results

Table I shows parameters for the experiment. In order to confirm the validity of the proposed method, a 2.3-kW prototype of the DAB converter was tested.

Figure 13 shows the operation waveforms of the conventional two-level mode and the proposed three-level mode. In the conventional two-level mode, the error of the transmission power of 21.5% occurs owing to the voltage polarity reverse phenomenon. In contrast, in Fig. 13 (b), the error of the transmission power is reduced by 20.8% by applying the proposed method because the voltage polarity reverse phenomenon is eliminated. Furthermore, the voltage polarity reverse phenomenon is also avoided in the three-level mode I. The error of the transmission power is reduced to 2.0% in the three-level mode I.

Figure 14 shows the transmission power characteristic. The non-linear error of the transmission power occurs due

Table I . Experimental parameters.

Quantity	Symbol	Value
Input voltage	V_{in}	240 V
Output voltage	V_{out}	240 V
Rated power	P	2.3 kW(45 deg)
Dead time	T_{dt}	2.1 μs (15 deg)
Auxiliary inductance	L	116 μH
Output capacitance	C	35 μF
Turn ratio of transformer	N	1
Switching frequency	f_{sw}	20 kHz
Margin of dead time	α	0.36 deg
Phase-shift of maximum power	δ_{max}	54.7 deg
Phase-shift of minimum power	δ_{min}	16.2 deg

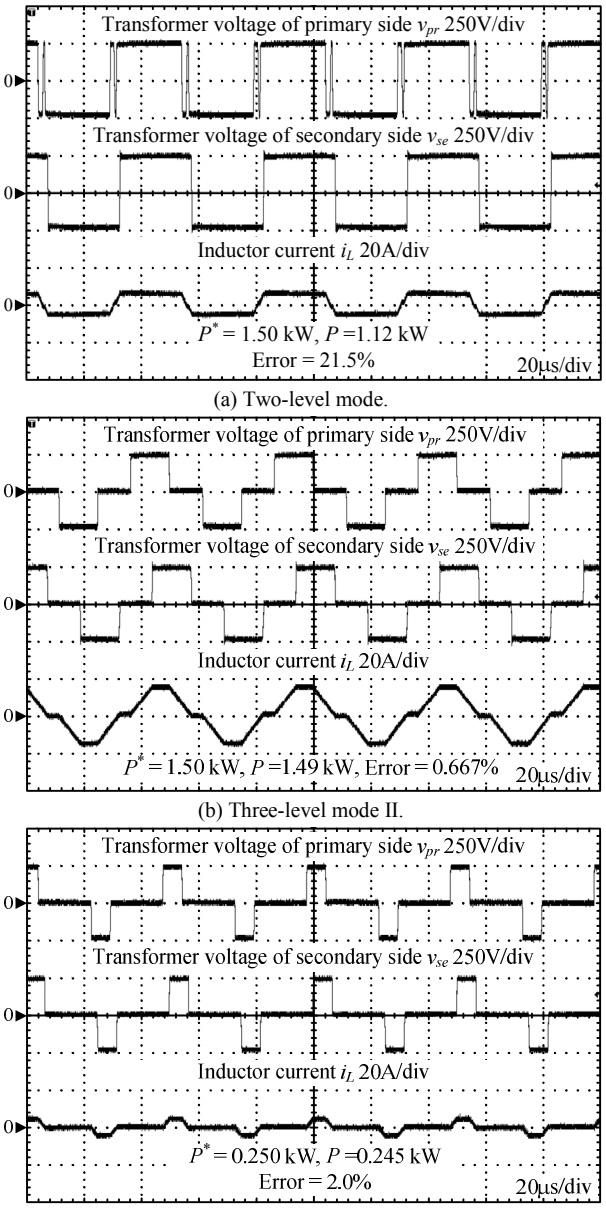

Fig. 13. Operation waveforms of two-level mode and proposed three-level mode.

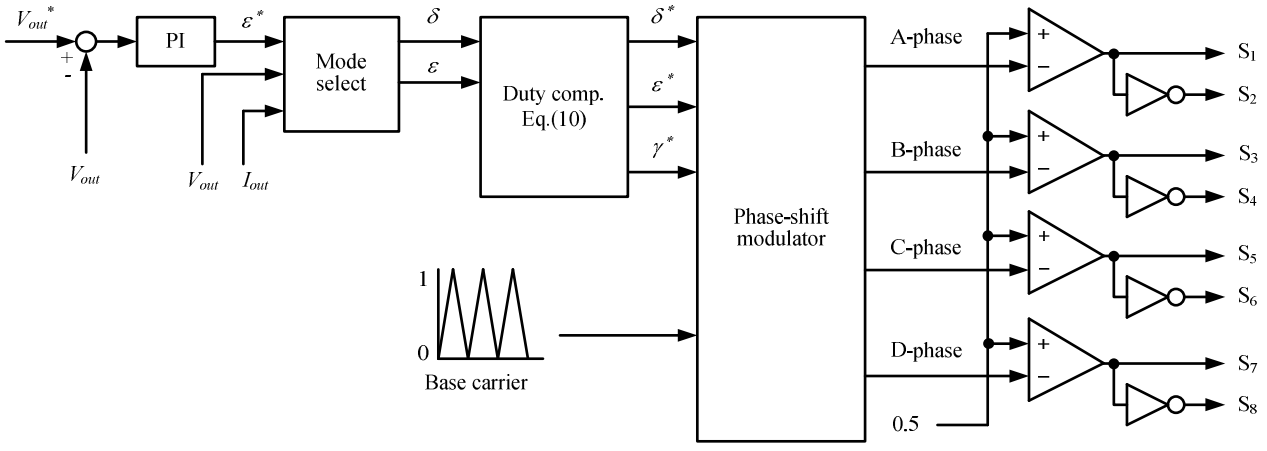

Fig. 12. Control block diaglam of proposed method.

to the voltage polarity reverse phenomenon when the two-level mode is used. On the other hand, the error of the transmission power is reduced by up to 76.3% using the proposed method.

Figure 15 shows the RMS value of the inductor current in the TRM and the TZM when the transmission power command is 0.50 kW. In the TRM, the RMS value of the inductor current is 6.12 A. As the result, the efficiency of the TRM is 85.3%. In contrast, using the TZM, the RMS value of the inductor current is reduced to 3.05 A, resulting the efficiency improvement to 93.8%. In the other words, the efficiency is improved by 8.5% because the RMS value of inductor current is reduced by 50.2%.

Figure 16 shows the characteristics between the transmission power and the RMS value of the inductor current in the TRM and the proposed TZM. By applying the proposed method, the RMS value of the inductor current is reduced by up to 54.0%. In the proposed three-level operation, the peak value of the inductor current depends on the phase-shift δ which is expressed by (5) of the interval $\varepsilon + \delta \leq \theta \leq \pi - \varepsilon$. Therefore, the RMS value of the inductor current in the three-level mode II is larger than the three-level mode I.

Figure 17 shows the characteristics between the zero-voltage period ε and the transmission power P. The transmission power fits with 2.3% of maximum error by controlling the zero current period to the dead-time or more. In addition, the DAB converter is controlled by the zero voltage period ε without the non-linear effect because the relationship between the zero voltage period ε and the output current is linear.

Figure 18 shows the load step dynamic response of proposed three-level operation with the voltage control when the load is changed from 0.43p.u. to 0.22p.u. This changing mode is conducted between two modes. In Fig. 18, the changing mode is achieved without the dc offset in the inductor current.

VI. Conclusion

This paper proposed the voltage control method for the DAB converter in the dead-time effect region with the three-level operation. This paper overcome two types of the non-linear effect in the DAB converter. Firstly, the non-linear error on the transmission power due to the voltage polarity reverse phenomenon was reduced by the three-level mode. The voltage polarity reverse phenomenon was eliminated by controlling the zero current period to the dead-time or more because the voltage polarity reversed phenomenon occurred when the inductor current reached zero during the dead-time. Secondly, the non-linearity between the manipulated variable and the DAB output current improved using the three-level operation. The three-level operation was operated by the zero voltage period with the constant value of the phase-shift. From the experimental results, the non-linear transmission power error was reduced by 76.3% because the voltage polarity reverse phenomenon was eliminated. In addition, the RMS value of the inductor current was reduced by 50.2% compared with the conventional TRM. As the results, the efficiency was improved by 8.5% because the conduction loss was reduced. Furthermore, the linearity between a control variable and an output current was confirmed. The transmission power fitted with the maximum error of 2.3%. Moreover, the load step between two three-level operations was achieved without the dc offset in the inductor current. In the future work, voltage control

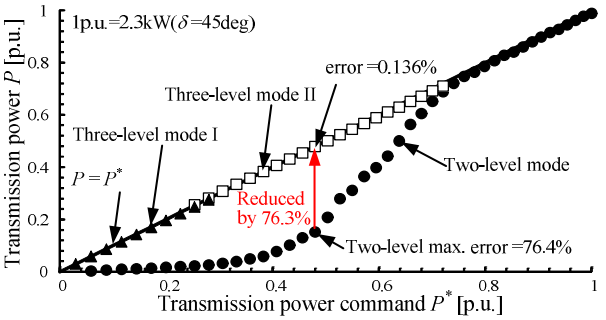

Fig. 14. Transmission power characteristic.

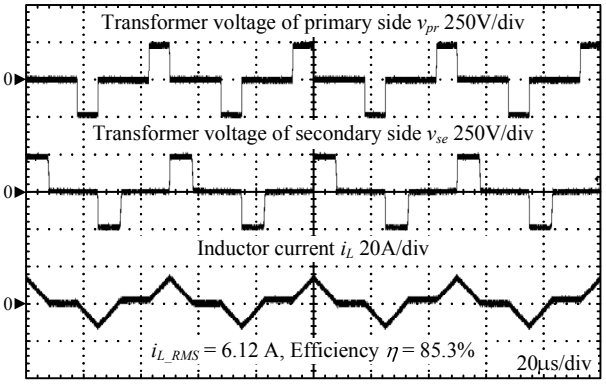

(a) TRM.

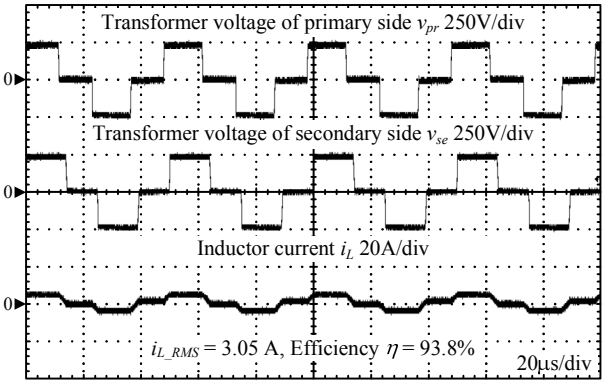

(b) TZM.

Fig. 15. RMS value of inductor current in TRM and TZM.

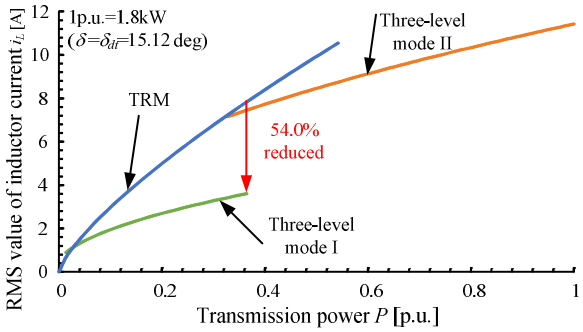

Fig. 16. Characteristics between transmission power and RMS value of inductor current.

method in the condition of $V_{in} \neq V_{out}$ will be considered.

REFERENCES

[1] M. Mao, Z. Dong, L. Chang: "Accurate Output Power Control of Converters for Microgrids Based on Local Measurement and Unified Control", IEEJ Journal of Industry Applications, Vol. 4, No. 4, pp.331-338, 2015.

[2] T. Tanaka, Y. Takahashi, K. Natori, and Y. Sato"High-Efficiency Floating Bidirectional Power Flow Controller for Next-Generation DC Power Network," IEEJ J. Industry Applications, vol. 7, no. 1, pp. 29-34, 2018.

[3] J. M. Guerrero, J. C. Vasquex, J. Matas, L. G. Vicuna, M. Castilla: "Hierarchical Control of Droop-Controlled AC and DC Microgrids—A General Approach Toward Standardization", IEEE Trans. on Industry Applications, Vol. 58, No. 1, pp.158-172, 2011.

[4] X. Liu, P. Wang and P. C. Loh, "A Hybrid AC/DC Microgrid and Its Coordination Control," in IEEE Transactions on Smart Grid, vol. 2, no. 2, pp. 278-286, June 2011.

[5] B. Zhao, Q. Song, W. Liu and Y. Xiao, "Next-Generation Multi-Functional Modular Intelligent UPS System for Smart Grid," in IEEE Transactions on Industrial Electronics, vol. 60, no. 9, pp. 3602-3618, Sept. 2013.

[6] Z. Zhang, Y. Cai, Y. Zhang, D. Gu and Y. Liu, "A Distributed Architecture Based on Microbank Modules With Self-Reconfiguration Control to Improve the Energy Efficiency in the Battery Energy Storage System," in IEEE Transactions on Power Electronics, vol. 31, no. 1, pp. 304-317, Jan. 2016.

[7] Y. Lu, Q. Wu, Q. Wang, D. Liu and L. Xiao, "Analysis of a Novel Zero-Voltage-Switching Bidirectional DC/DC Converter for Energy Storage System," in IEEE Transactions on Power Electronics, vol. 33, no. 4, pp. 3169-3179, April 2018.

[8] M. Tariq, A. I. Maswood, C. J. Gajanayake and A. K. Gupta, "Modeling and Integration of a Lithium-Ion Battery Energy Storage System With the More Electric Aircraft 270 V DC Power Distribution Architecture," in IEEE Access, vol. 6, pp. 41785-41802, 2018.

[9] V. Karthikeyan and R. Gupta, "Multiple-Input Configuration of Isolated Bidirectional DC–DC Converter for Power Flow Control in Combinational Battery Storage," in IEEE Transactions on Industrial Informatics, vol. 14, no. 1, pp. 2-11, Jan. 2018.

[10] R. W. A. A. De Doncker, D. M. Divan and M. H. Kheraluwala, "A three-phase soft-switched high-power-density DC/DC converter for high-power applications," in IEEE Transactions on Industry Applications, vol. 27, no. 1, pp. 63-73, Jan.-Feb. 1991.

[11] M. N. Kheraluwala, R. W. Gascoigne, D. M. Divan and E. D. Baumann, "Performance characterization of a high-power dual active bridge DC-to-DC converter," in IEEE Transactions on Industry Applications, vol. 28, no. 6, pp. 1294-1301, Nov.-Dec. 1992.

[12] G. Guidi, A. Kawamura, Y. Sasaki and T. Imakubo, "Dual active bridge modulation with complete zero voltage switching taking resonant transitions into account," Proceedings of the 2011 14th European Conference on Power Electronics and Applications, Birmingham, 2011, pp. 1-10.

[13] D. Nguyen, D. T. Nguyen, and G. Fujita, "New Modulation Strategy Combining Phase Shift and Frequency Variation for Dual-Active-Bridge Converter", IEEJ J. Industry Applications, vol.6, no.2, pp.140-150, 2017.

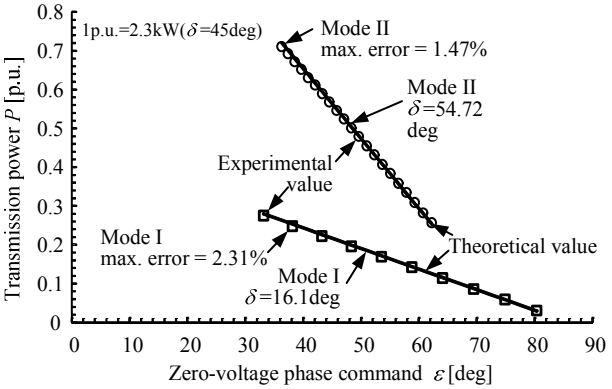

Fig. 17. Characteristics between zero-voltage period and transmission power.

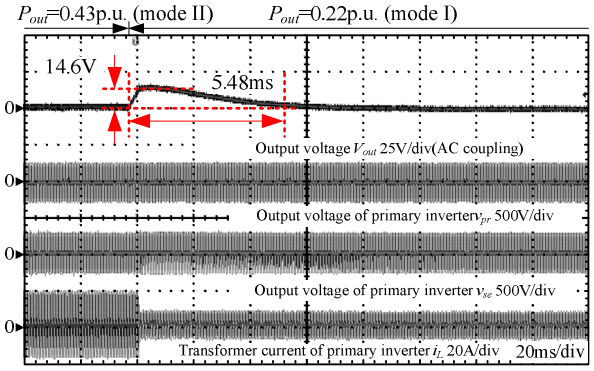

Fig. 18. Load step dynamic response of proposed three-level operation.

[14] M. H. A. b. A. Malek, H. Kakigano, and K. Takaba"Combined Pulse-Width Modulation of Dual Active Bridge DC-DC Converter to Increase the Efficiency of Bidirectional Power Transfer,"IEEJ J. Industry Applications, vol. 7, no. 2, pp. 166-174, 2018.

[15] H. Higa and J. Itoh, "Extension of zero-voltage-switching range in dual active bridge converter by switched auxiliary inductance," 2017 IEEE Energy Conversion Congress and Exposition (ECCE), Cincinnati, OH, 2017, pp. 5324-5331.

[16] K. Takagi and H. Fujita, "Dynamic control and dead-time compensation method of an isolated dual-active-bridge DC-DC converter," 2015 17th European Conference on Power Electronics and Applications (EPE'15 ECCE-Europe), Geneva, 2015, pp. 1-10.

[17] D. Segaran, D. G. Holmes and B. P. McGrath, "Enhanced Load Step Response for a Bidirectional DC–DC Converter," in IEEE Transactions on Power Electronics, vol. 28, no. 1, pp. 371-379, Jan. 2013.

[18] B. Zhao, Q. Song, W. Liu, Y. Sun: "Dead time Effect of the High-Frequency Isolated Bidirectional Full-Bridge DC-DC Converter: Comprehensive Theoretical Analysis and Experimental Verification", IEEE Trans. on Power Electronics, Vol. 29, No. 4, pp.1667-1680, 2014.

[19] J. Itoh, K. Kawauchi, H. Higa " Dead-time Compensation with DC Offset Current Elimination Method using Three-level Operation for Dual Active Bridge DC-DC Converter," 2018 IEEE Energy Conversion Congress and Exposition (ECCE), Portland, OR, pp. 6299-6306, 2018.

[20] H. Zhou, A. M. Khambadkone: "Hybrid Modulation for Dual-Active-Bridge Bidirectional Converter With Extended Power Range for Ultracapacitor Application", IEEE Trans. on Industry Application, Vol. 29, No. 4, pp.1667-1680, 2014.

[21] J.-J. Slotine, W. Li, Applied Nonlinear Control, NJ, Englewood Cliffs:Prentice-Hall, Oct. 1990.